anism may partly compensate for the minor spliceosome deficiency resulting from mutations in *U4atac* snRNA.

This paper shows compelling evidence that mutations in the *U4atac* snRNA gene are responsible for the early postnatal sudden death and severe brain and bone malformations seen in TALS, through minor spliceosome deficiency. Decreased expression of a restricted number of U12 genes and subsequent effects on downstream metabolic pathways may explain the TALS phenotype.

References and Notes

1. H. Taybi, D. Linder, *Radiol. Easton PA* **89**, 275 (1967).
2. S. Sigaudy *et al.*, *Am. J. Med. Genet.* **80**, 16 (1998).
3. A. L. Leutenegger *et al.*, *Am. J. Hum. Genet.* **79**, 62 (2006).
4. A. L. Leutenegger *et al.*, *Am. J. Hum. Genet.* **73**, 516 (2003).
5. W. Y. Tarn, J. A. Steitz, *Science* **273**, 1824 (1996).
6. W. Y. Tarn, J. A. Steitz, *Cell* **84**, 801 (1996).
7. R. A. Padgett, G. C. Shukla, *RNA (N.Y.)* **8**, 125 (2002).
8. S. Nottrott *et al.*, *EMBO J.* **18**, 6119 (1999).
9. I. Vidovic, S. Nottrott, K. Hartmuth, R. Luhrmann, R. Ficner, *Mol. Cell* **6**, 1331 (2000).
10. G. C. Shukla, A. J. Cole, R. C. Dietrich, R. A. Padgett, *Nucleic Acids Res.* **30**, 4650 (2002).
11. S. Nottrott, H. Urlaub, R. Luhrmann, *EMBO J.* **21**, 5527 (2002).
12. S. Liu *et al.*, *Science* **316**, 115 (2007).
13. A. Schultz, S. Nottrott, K. Hartmuth, R. Luhrmann, *J. Biol. Chem.* **281**, 28278 (2006).
14. A. Levine, R. Durbin, *Nucleic Acids Res.* **29**, 4006 (2001).
15. T. S. Alioto, *Nucleic Acids Res.* **35** (database), D110 (2007).
16. P. A. Sharp, C. B. Burge, *Cell* **91**, 875 (1997).
17. M. W. Hentze, A. E. Kulozik, *Cell* **96**, 307 (1999).
18. Y. F. Chang, J. S. Imam, M. F. Wilkinson, *Annu. Rev. Biochem.* **76**, 51 (2007).
19. L. R. Otake, P. Scamborova, C. Hashimoto, J. A. Steitz, *Mol. Cell* **9**, 439 (2002).
20. H. K. Pessa *et al.*, *PLoS ONE* **5**, e13215 (2010).

21. We express our heartfelt thanks to the patients and families who participated in this study. We thank M. Gallagher-Gambarelli for her editorial assistance and R. Hennekam for his assistance during the project; M. Letexier for her assistance in analyzing high-throughput sequencing data; T. Rio Frio for helpful discussions on splicing analyses; M. de Tayrac and C. Depienne for helpful discussions on expression data analysis; I. Rouvet and M.-T. Zabot for fibroblast banking; and R. Padgett for providing us with the hand-built *U4atac*/*U6atac* bimolecular structure reflecting mfold software predictions. This work was supported by the Fondation Yves Cotrel-Institut de France, the Hospices Civils de Lyon, the French Ministry of Health (Direction de l'Hospitalisation et de l'Organisation des Soins, Plan Maladies Rares 2004), Lyon 1 University, the INSERM, the Association GEN'HOM, and the Texas Scottish Rite Hospital for Children Research Fund.

Supporting Online Material

www.sciencemag.org/cgi/content/full/332/6026/240/DC1
Materials and Methods
SOM Text
Figs. S1 to S8
Tables S1 to S4
References

27 December 2010; accepted 3 March 2011
10.1126/science.1202205

Eosinophils Sustain Adipose Alternatively Activated Macrophages Associated with Glucose Homeostasis

Davina Wu,[1] Ari B. Molofsky,[2] Hong-Erh Liang,[1] Roberto R. Ricardo-Gonzalez,[3] Hani A. Jouihan,[3] Jennifer K. Bando,[1] Ajay Chawla,[4] Richard M. Locksley[1,5,6]*

Eosinophils are associated with helminth immunity and allergy, often in conjunction with alternatively activated macrophages (AAMs). Adipose tissue AAMs are necessary to maintain glucose homeostasis and are induced by the cytokine interleukin-4 (IL-4). Here, we show that eosinophils are the major IL-4–expressing cells in white adipose tissues of mice, and, in their absence, AAMs are greatly attenuated. Eosinophils migrate into adipose tissue by an integrin-dependent process and reconstitute AAMs through an IL-4– or IL-13–dependent process. Mice fed a high-fat diet develop increased body fat, impaired glucose tolerance, and insulin resistance in the absence of eosinophils, and helminth-induced adipose tissue eosinophilia enhances glucose tolerance. Our results suggest that eosinophils play an unexpected role in metabolic homeostasis through maintenance of adipose AAMs.

Adipose tissue macrophages have a central role in promoting chronic low-grade inflammation, which contributes to obesity, insulin resistance, and type 2 diabetes, which characterize the metabolic syndrome (*1*). Although adipose macrophages from obese animals have a classically activated inflammatory phenotype, adipose macrophages from healthy lean mice have an alternatively activated phenotype (*2*). Impeding the ability of macrophages to become alternatively activated by disrupting the nuclear hormone receptor peroxisome proliferator-activated receptor-γ (PPARγ) renders mice susceptible to diet-induced obesity and glucose intolerance (*3*, *4*). Human PPARγ loss-of-function mutations are also associated with insulin resistance and type 2 diabetes (*5*). PPARγ is induced in macrophages by interleukin-4 (IL-4) or IL-13 and promotes arginase-1 expression, one of the signature genes in alternatively activated macrophages (AAMs) (*6*). In vitro studies with adipocyte cell lines suggest that adipocytes themselves can be sources of IL-4 and IL-13 (*7*), but analysis of adipose tissues in vivo are needed to ascertain more definitively the source of these cytokines.

To begin an unbiased analysis of IL-4–expressing cells in perigonadal white adipose tissue of mice fed a normal commercial diet, we used IL-4 reporter mice (4get mice) (*8*), which contain a green fluorescent protein (GFP) reporter downstream of an internal ribosomal entry site element after the endogenous *Il4* gene, which facilitates recognition of IL-4–competent cells in vivo as revealed by their fluorescence (*9*). To ensure minimal manipulation, we first analyzed cells spontaneously migrating out of minced adipose tissue after overnight incubation in medium. Although only small numbers of IL-4–expressing (GFP+) CD4+ T cells could be recovered, a large population of GFP+ eosinophils, which constitutively express GFP in 4get mice (*9*, *10*), were identified (fig. S1A). We next enzymatically digested perigonadal adipose tissue to prepare a stromal vascular fraction (SVF) and recovered all IL-4–expressing cells for analysis. Of the IL-4–competent cells recovered from perigonadal adipose tissue of mice fed a normal diet, 90% were eosinophils, with the remainder made up of small numbers of basophils, CD4+ T cells, and innate helper type 2 cells (Fig. 1A, eosinophil gating in fig. S1B). Similar to the relatively abundant adipose tissue macrophages, adipose tissue eosinophils were CD11b+ F4/80+ but were distinguished both by GFP expression in 4get mice and by expression of the sialic acid–binding immunoglobulin receptor, Siglec-F (fig. S1, B and C). Analysis of adipose tissues from 4get mice with a *Gata1* promoter mutation that lack eosinophils (ΔdblGATA mice) (*11*) confirmed that the isolated cells were eosinophils (fig. S1D). Using mice with a knock-in human *CD2* replacement gene at the *il4* start site to mark cells that have recently secreted IL-4 protein (*10*), we could show that the majority of IL-4–secreting cells in adipose tissue were eosinophils, although the number of IL-4–secreting cells was only a small proportion of the total GFP+ IL-4–competent cells (fig. S2). Eosinophils up-regulate the inhibitory Siglec-F receptor as they move from blood into tissues (*12*). Compared with blood eosinophils, adipose tissue eosinophils show increased Siglec-F expression, consistent with tissue residence (fig. S1E). Eosinophils account for 4 to 5% of the adipose SVF cells, more abundant than total adipose CD4+ T cells (fig. S1F) or eosinophils in spleen (0.33% ± 0.08%, mean % viable cells ± SEM) or blood (2.4% ± 0.4%, mean ± SEM). Examination of perigonadal adipose tissue by

[1]Howard Hughes Medical Institute, University of California, San Francisco, San Francisco, CA 94143–0795, USA. [2]Department of Laboratory Medicine, University of California, San Francisco, San Francisco, CA 94143, USA. [3]Division of Endocrinology, Metabolism, and Gerontology, Department of Medicine, Stanford University School of Medicine, Stanford, CA 94305–5103, USA. [4]Cardiovascular Research Institute and Departments of Physiology and Medicine, University of California, San Francisco, San Francisco, CA 94107, USA. [5]Department of Medicine, University of California, San Francisco, San Francisco, CA 94143, USA. [6]Department of Microbiology and Immunology, University of California, San Francisco, San Francisco, CA 94143, USA.

*To whom correspondence should be addressed. E-mail: locksley@medicine.ucsf.edu

standard histochemistry from wild-type (WT) mice identified eosinophils in normal perigonadal fat (Fig. 1B). Flow cytometric and immunohistochemical examination of adipose tissue from WT, eosinophil-deficient, and hypereosinophilic IL-5 transgenic (IL-5tg) mice (*13*) confirmed that Siglec-F–positive cells with the appearance of eosinophils were present in adipose tissue in numbers that correlated with the eosinophil status of the mice (Fig. 1, C and D). Eosinophils were also identified in perigonadal adipose tissue from WT C57BL/6 mice (Fig. 1, E and F). We noted a reciprocal relation between adipose tissue eosinophils and adiposity, as eosinophils were present but reduced in frequency in C57BL/6 mice fed a high-fat diet (Fig. 1, E and F) or in mice with genetic obesity secondary to leptin deficiency (*ob/ob*) (fig S3, A and B), and adipose tissue eosinophil numbers correlated inversely with mouse weight (Fig. 1, G and H). Tissue eosinophils with up-regulated Siglec-F were present in perigonadal, subcutaneous, mesenteric, and brown adipose tissues; however, the frequency and absolute eosinophil numbers were highest in the metabolically active perigonadal and mesenteric adipose tissues (fig. S3, C and D), with the highest percentage of CD11b+ F4/80+ macrophages [perigonadal 32.4 ± 3.5%; mesenteric 20.7 ± 5.3%; brown 13.8 ± 2.3%; and subcutaneous 1.2 ± 0.08% (mean ± SEM)].

To determine whether eosinophils migrate into adipose tissue, we transferred splenic eosinophils from hypereosinophilic mice (IL-5tg × 4get) to eosinophil-deficient mice. After 3 days, eosinophils were recovered from lung, spleen, and perigonadal fat. By 7 days, however, when eosinophils had declined substantially in lung and spleen, eosinophils remained in stable numbers in adipose tissue (Fig. 2A) and in small intestine (fig. S4). Adoptively transferred eosinophils recovered from adipose tissue up-regulated Siglec-F, consistent with their tissue residence and distinct from the lower amounts of Siglec-F on spleen eosinophils harvested at the same time (fig. S5A). To confirm that eosinophil migration required transit from the blood to adipose tissue, we compared eosinophil accumulation in tissues of mice treated with antibodies that block vascular cell adhesion molecule–1 and intercellular cell adhesion molecule–1–mediated migration through α_4 and α_L integrins expressed on eosinophils (*14*). As compared with animals receiving isotype control antibodies, treatment with antibodies against integrin blocked accumulation of eosinophils in adipose tissues (Fig. 2B). Con-

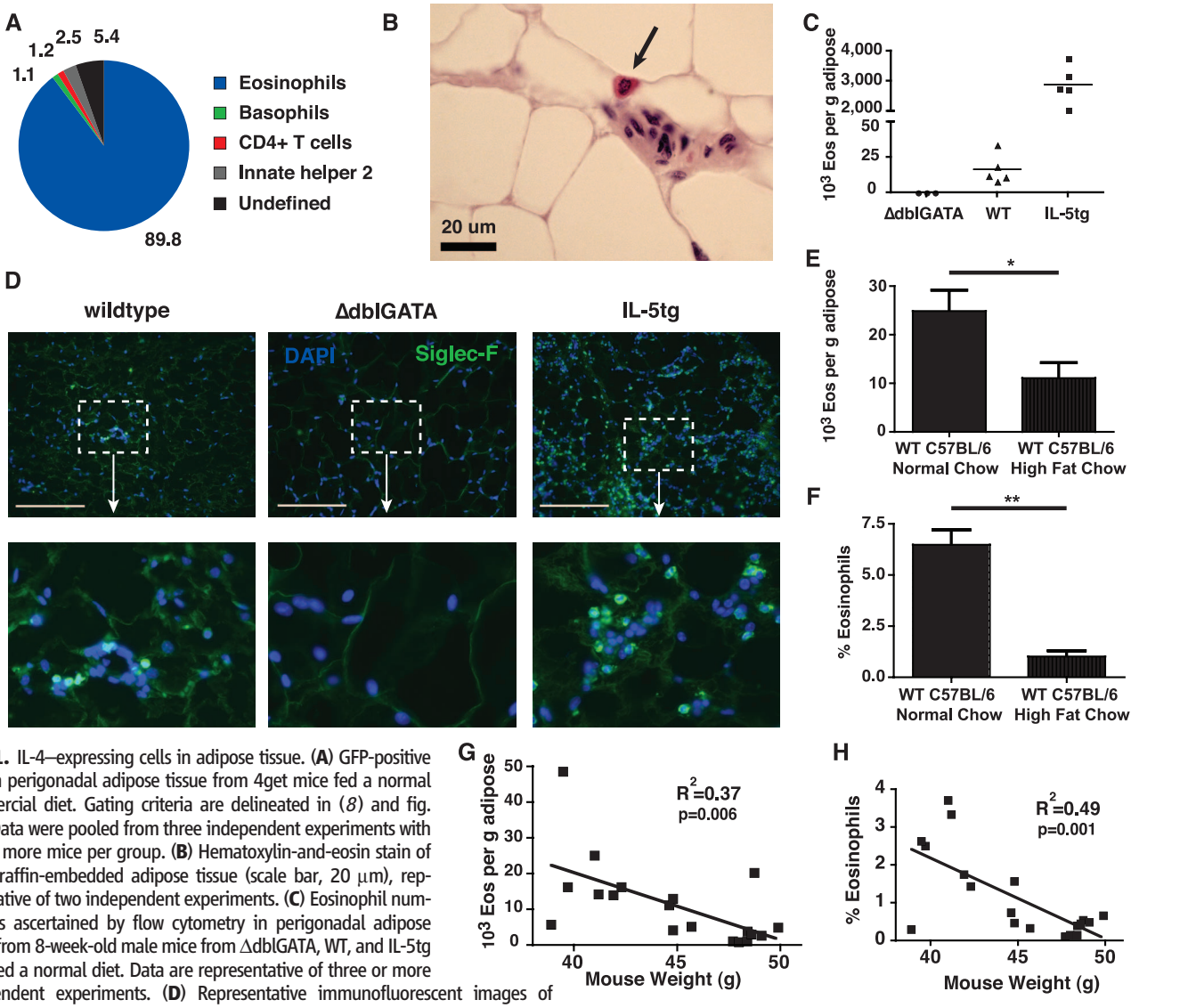

Fig. 1. IL-4–expressing cells in adipose tissue. (**A**) GFP-positive cells in perigonadal adipose tissue from 4get mice fed a normal commercial diet. Gating criteria are delineated in (*8*) and fig. S1B. Data were pooled from three independent experiments with two or more mice per group. (**B**) Hematoxylin-and-eosin stain of WT paraffin-embedded adipose tissue (scale bar, 20 μm), representative of two independent experiments. (**C**) Eosinophil numbers as ascertained by flow cytometry in perigonadal adipose tissue from 8-week-old male mice from ΔdblGATA, WT, and IL-5tg mice fed a normal diet. Data are representative of three or more independent experiments. (**D**) Representative immunofluorescent images of Siglec-F+ cells in perigonadal adipose tissue from the strains indicated (scale bar, 50 μm). Siglec-F, green; nuclei counterstain with 4′,6′-diamidino-2-phenylindole (DAPI), blue; representative of two experiments. (**E** to **H**) WT male C57BL/6 mice were fed a high-fat diet (HF Chow) for 10 to 14 weeks and compared with WT C57BL/6 controls mice fed a normal diet (normal Chow). Perigonadal adipose tissue eosinophils were quantified by flow cytometry (E) per g adipose tissue or (F) percentage of total SVF cells. Correlation is shown between the weight of mice fed a high-fat diet and their adipose tissue eosinophil numbers (G and H), by using Pearson's correlation coefficient. (E to H) Results are pooled data from two independent experiments with 20 total mice. *$P < 0.05$; **$P < 0.01$.

versely, in lung and spleen, where most eosinophils retain low Siglec-F expression and presumably remain within the abundant vasculature of these organs, eosinophils accumulated in animals treated with the integrin-specific antibodies. Integrin-specific antibodies similarly blocked eosinophil migration into adipose tissue after induction of endogenous eosinophilia by IL-25 administration (*15*) (fig. S5, B and C).

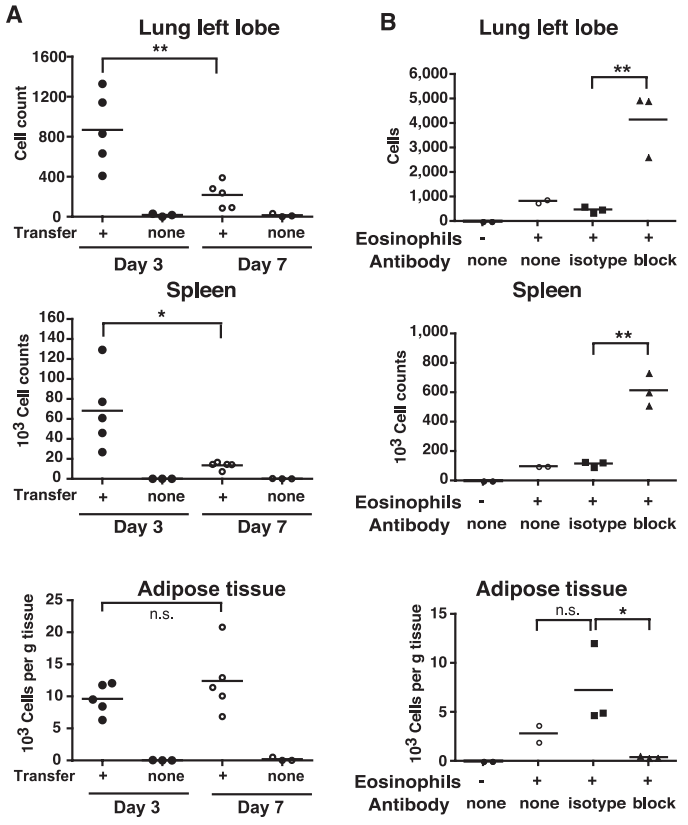

Fig. 2. Eosinophil migration to adipose tissue is integrin-mediated. (**A**) Eosinophils in the left lobe of the lung, spleen, and perigonadal adipose tissue 3 and 7 days after adoptive transfer into eosinophil-deficient ΔdblGATA mice fed a normal diet. Data are pooled from two independent experiments. (**B**) ΔdblGATA mice received antibodies to α_4 and α_L integrins (100 μg each) that block migration or control isotypes of immunoglobulin G (IgG2a and IgG2b) 2 hours before adoptive transfer of eosinophils. Tissues were harvested 16 hours later. Data are representative of two independent experiments. *$P < 0.05$; **$P < 0.01$ as determined with Student's *t* test. n.s., not significant.

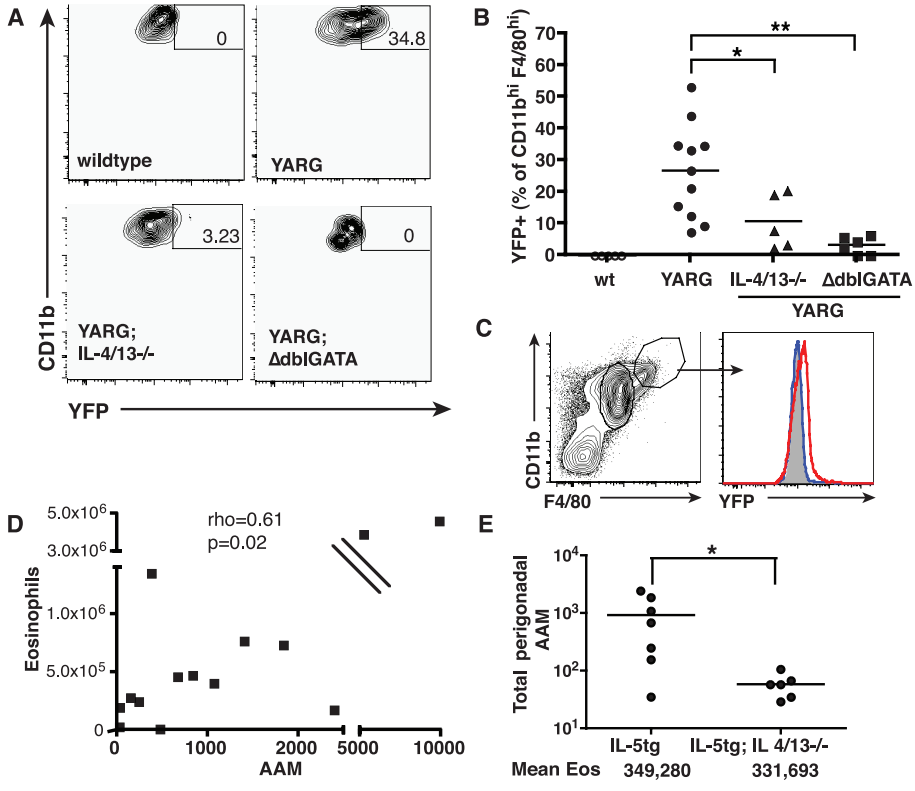

Fig. 3. Adipose macrophage alternative activation is impaired in the absence of IL-4 and IL-13 or eosinophils. (**A**) Flow cytometric analysis of adipose tissue from indicated mice fed a normal diet. Gates show YFP-positive cells as a percentage of total CD11b^{high} F4/80^{high} macrophages (A) and are quantified (**B**). Results are pooled data from two or more independent experiments with two to four animals per experiment. *$P < 0.05$; **$P < 0.01$ as determined using analysis of variance (ANOVA) with Bonferroni's posttest correction for multiple comparisons. (**C**) ΔdblGATA × YARG mice were sublethally irradiated and reconstituted with bone marrow cells from 4get × IL-5tg mice. After 4 to 6 weeks, perigonadal adipose tissues were analyzed for eosinophils (left gate; eosinophils were GFP-positive and side-scatter^{high}, not shown) and macrophages (CD11b^{high} F4/80^{high}, right gate). Macrophages were then analyzed for YFP. Eosinophil-reconstituted mice (red); nonreconstituted mice (blue); WT control (nonreporter) mice (gray). (**D**) Statistical correlation (Spearman's rank correlation) between the total numbers of eosinophils reconstituting perigonadal adipose tissues in eosinophil-deficient mice and the total numbers of AAMs expressing the marker arginase-1 allele. Results are pooled data from five independent experiments with two to four animals per experiment. (**E**) Mice reconstituted with IL-5tg bone marrow lacking IL-4 and IL-13 (IL-5tg; IL 4/13-/-) display significantly fewer total YARG+ AAMs (E) or total YARG+ AAMs per 1000 tissue eosinophils (IL-5tg 2.5 ± 1.1; IL-5tg × 4/13 DKO 2.4 × 10^{-4} ± 6.2 × 10^{-5}). Results are pooled data from two or more independent experiments with two to five animals per experiment. *$P < 0.05$; **$P < 0.01$ as determined using Student's *t* test.

Studies of AAMs in adipose tissue have relied on polymerase chain reaction–based detection of signature genes in order to confirm the presence of these cells, but single-cell analysis has not been possible. Arginase-1 is a signature gene in mouse AAMs that is induced by IL-4 (*6*). We isolated cells in perigonadal fat from YARG mice, which have a fluorescent reporter introduced into the *arg-1* gene, that can used to identify AAMs in vivo (*16*) (fig. S6). In both WT and YARG mice fed a normal diet, total numbers of CD11b+ F4/80+ macrophages were similar in adipose tissue (fig. S7), and in YARG mice, yellow fluorescent protein–positive (YFP+) macrophages were detected without further manipulation (Fig. 3A and fig. S7A). We used size-gating and Siglec-F expression to confirm that eosinophils do not express YFP fluorescence in YARG mice (fig. S7B). In the absence of IL-4 and IL-13 (*17*), numbers of total adipose macrophages remained similar (fig. S7C), but numbers of arginase-1–expressing macrophages diminished significantly (Fig. 3, A and B), consistent with a role for these cytokines in sustaining the phenotype of adipose AAMs under homeostatic conditions and in agreement with prior studies using Stat6-deficient mice (*3*). Contrary to our expectations, adipose tissues from YARG mice that had been crossed onto the eosinophil-deficient background (YARG × ΔdblGATA) also demonstrated a significant reduction of AAMs in adipose tissue (Fig. 3, A and B), with similar numbers of total macrophages (fig. S7C). To ascertain whether eosinophils are sufficient to sustain AAMs in adipose tissue, we sublethally irradiated eosinophil-deficient YARG mice and reconstituted them with bone marrow cells from hypereosinophilic mice (IL-5tg × 4get). After 4 to 6 weeks, the perigonadal adipose tissues from reconstituted mice contained GFP+ eosinophils and YFP+ AAMs that were not present in nonreconstituted eosinophil-deficient mice (Fig. 3C). The numbers of eosinophils recovered within the perigonadal adipose tissue of the reconstituted mice correlated with the numbers of arginase-1–expressing macrophages in the same tissue (Fig. 3D). In contrast, animals reconstituted with IL-5tg bone marrow lacking IL-4 and IL-13 (double knockout) (IL-5tg × 4/13 DKO) had similar numbers of spleen and adipose tissue eosinophils, as well as similar adipose tissue weights, but did not restore AAMs (Fig. 3E and fig S8, A and B). Thus, eosinophils and hematopoietic cell-derived IL-4–IL-13 are required to sustain adipose AAMs. Supporting these experiments, IL-4 and IL-13 transcripts were found predominantly in the SVF rather than the adipocyte fraction of perigonadal white adipose tissue from WT mice (fig. S8, D and E).

During these experiments, it became apparent that the visceral adipose tissue of hypereosinophilic IL-5tg mice was visually smaller than the same tissues from littermate WT mice when both were fed a normal diet (Fig. 4A). As compared with WT mice, IL5tg mice had an improved response to a glucose challenge (Fig. 4B). Although differences in adipose tissue weight were not significant in eosinophil-deficient mice maintained on a normal diet, adiposity was greatly augmented when the mice were fed a high-fat diet. Under these conditions, analysis with dual-energy x-ray absorptiometry (DEXA) scans demonstrated significant increases in total body fat and percentage fat content in eosinophil-deficient mice as compared with WT littermates maintained on a high-fat diet, which suggested a role for eosinophils in protecting against diet-induced obesity (Fig. 4, C and D). The obesity induced in eosinophil-deficient mice fed a high-fat diet was metabolically relevant, because these mice demonstrated significantly impaired glucose tolerance compared with WT animals (Fig. 4E). When aged to 20 to 24 weeks while being maintained on a high-fat diet,

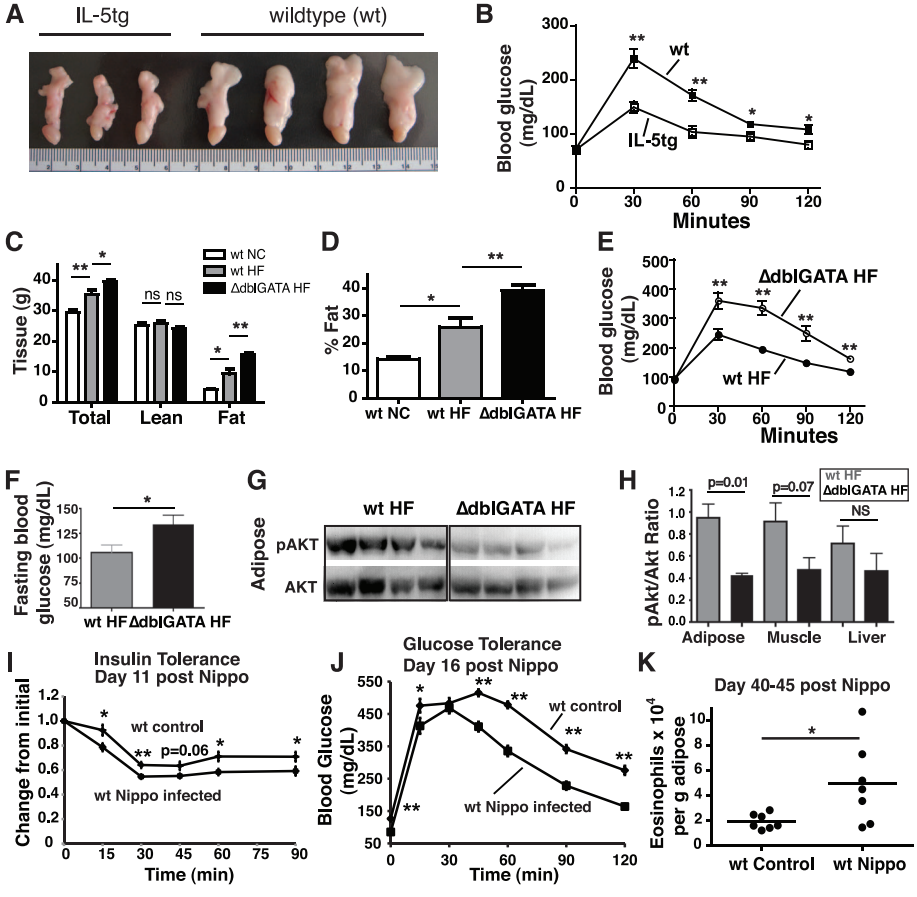

Fig. 4. Metabolic analysis of eosinophil-deficient and hypereosinophilic mice. (**A**) Perigonadal fat tissues (testis attached) from IL-5 transgenic (IL-5tg) and WT littermate controls. (**B**) Fasting male 8-week-old WT or IL-5tg littermates maintained on a normal commercial (NC) diet were challenged with intraperitoneal glucose, and blood was sampled for glucose at times indicated. Data were compiled from two independent experiments with six or seven mice in each group. (**C** and **D**) DEXA analysis of total, lean, and fat tissue composition (C) or percentage adiposity (D) in ΔdblGATA and WT mice fed an NC or high-fat (HF) diet for 15 weeks. Data were compiled from two experiments with five to eight mice in each group. (**E**) Intraperitoneal glucose tolerance test in male ΔdblGATA and WT mice fed HF diet for 15 weeks. Data were compiled from three independent experiments with five to eight mice in each group. (**F**) Fasting blood glucose in male WT and ΔdblGATA mice maintained on a HF diet for 20 to 22 weeks. Data were compiled from two independent experiments with five mice in each group. (**G** and **H**) Insulin signaling, as measured by the ratio of serine-phosphorylated Akt to total Akt in adipose tissue, muscle, and liver of mice aged 24 weeks fed a HF diet (n = four to six mice per genotype, four representative mouse adipose tissue samples shown). (**I** and **J**) Twelve-week old WT C57BL/6 mice fed a HF diet for 6 weeks were infected with *N. brasiliensis* (Nippo) or unchallenged (control) and monitored for (I) insulin tolerance and (J) glucose tolerance, at the indicated times. Insulin tolerance results are normalized to baseline fasting glucose, which was statistically different between cohorts (WT control 207 mg/dl ± 6; Nippo 179 mg/dl ± 7; $P < 0.05$). (**K**) Adipose tissue collected at days 40 to 45 post *N. brasiliensis* infection or from uninfected control mice and analyzed by flow cytometry for eosinophils per gram adipose tissue or percent eosinophils (WT control 2.9% ± 0.41; Nippo 10.1% ± 0.36, $P < 0.01$). Data (I, J, and K) are representative of two independent experiments with 20 to 30 total mice per cohort. *$P < 0.05$; **$P < 0.01$ as determined by Student's t test (B, E, and F, and H to K) or ANOVA with Bonferroni's posttest correction for multiple comparisons (C and D); error bars, SEM; n.s., not significant.

eosinophil-deficient mice had normal to mildly elevated levels of fasting insulin (fig. S9A), which indicated adequate pancreatic beta-cell insulin production. Eosinophil-deficient mice had elevated fasting blood glucose levels (Fig. 4F), however, and decreased adipose tissue insulin responsiveness, as shown by diminished tissue phosphorylated Akt levels after insulin challenge (Fig. 4, G and H).

To ask whether physiologic elevations of eosinophils could improve glucose tolerance in the setting of a high-fat diet, we infected mice fed a high-fat diet with a migratory helminth, *Nippostrongylus brasiliensis*. Although the parasite is cleared after 8 days, a sustained metabolic response was seen, characterized by decreased fasting glucose and improved insulin sensitivity and glucose tolerance present early post infection (Fig. 4, I and J) and sustained up to 35 days post infection (fig. S9B). Remarkably, decreased perigonadal adipose tissue weight (control 2.4 g ± 0.12; infected 1.8 g ± 0.15, $P < 0.01$) and increased perigonadal adipose tissue eosinophils were also maintained up to 45 days post infection (Fig. 4K), when spleen, liver, and bone marrow eosinophils had returned to baseline (fig. S9C). Total adipose macrophages from the infected cohort were also relatively decreased (control 50.6% ± 2.7; infected 35.3% ± 2.0, $P < 0.05$), consistent with a decline of classically activated macrophages known to preferentially populate adipose tissue during high-fat feeding (*2*).

Despite much literature defining a role for AAMs in sustaining insulin sensitivity and glucose homeostasis, the mechanisms responsible for maintaining these cells in healthy adipose tissues are largely unknown. Although differences exist between mouse and human AAMs, including in the expression of arginase-1 as used here, we note the overlapping profiles of IL-4- and IL-13–conditioned human monocyte/macrophages that have also allowed recognition of human AAMs (*6*). Our work suggests that eosinophil IL-4 production may contribute to sustaining AAMs; however, additional contributions from eosinophils are likely important, possibly through production of cytokines, chemokines, or other mediators. Furthermore, we note that innate helper 2 (ih2) cells, recently implicated as an important source of IL-5 and IL-13, are present in adipose tissues (Fig. 1A), as previously noted (*18*), and future study will be required to address whether cytokines from these cells maintain adipose tissue eosinophil homeostasis. Additional contributions by adaptive immune cells likely add further complexity and fine control (*19*–*21*).

Despite their appearance in allergy and states of parasitism, particularly in response to intestinal helminthes, the biologic role of eosinophils remains incompletely defined. Although sparse in blood of persons in developed countries, eosinophils are often elevated in individuals in rural developing countries where intestinal parasitism is prevalent and metabolic syndrome rare (*22*). We speculate that eosinophils may have evolved to optimize metabolic homeostasis during chronic infections by ubiquitous intestinal parasites (*23*), and in contrast to the insulin-resistant state induced by acute microbial infections (*24*). Our findings further support the intertwined relationship between metabolism and immunity (*1*) and are consistent with the enrichment of inflammatory and immune response genes associated with obesity in humans (*25*, *26*). Modulating adipose tissue eosinophil number and function could provide an exciting and novel therapeutic target in human metabolic disorders.

References and Notes

1. G. S. Hotamisligil, *Nature* **444**, 860 (2006).
2. C. N. Lumeng, J. L. Bodzin, A. R. Saltiel, *J. Clin. Invest.* **117**, 175 (2007).
3. J. I. Odegaard *et al.*, *Nature* **447**, 1116 (2007).
4. M. A. Bouhlel *et al.*, *Cell Metab.* **6**, 137 (2007).
5. E. H. Jeninga, M. Gurnell, E. Kalkhoven, *Trends Endocrinol. Metab.* **20**, 380 (2009).
6. F. O. Martinez, L. Helming, S. Gordon, *Annu. Rev. Immunol.* **27**, 451 (2009).
7. K. Kang *et al.*, *Cell Metab.* **7**, 485 (2008).
8. Materials and methods are available as supporting material on *Science* Online.
9. M. Mohrs, K. Shinkai, K. Mohrs, R. M. Locksley, *Immunity* **15**, 303 (2001).
10. K. Mohrs, A. E. Wakil, N. Killeen, R. M. Locksley, M. Mohrs, *Immunity* **23**, 419 (2005).
11. C. Yu *et al.*, *J. Exp. Med.* **195**, 1387 (2002).
12. D. Voehringer, N. van Rooijen, R. M. Locksley, *J. Leukoc. Biol.* **81**, 1434 (2007).
13. N. A. Lee *et al.*, *J. Immunol.* **158**, 1332 (1997).
14. M. E. Rothenberg, S. P. Hogan, *Annu. Rev. Immunol.* **24**, 147 (2006).
15. M. M. Fort *et al.*, *Immunity* **15**, 985 (2001).
16. T. A. Reese *et al.*, *Nature* **447**, 92 (2007).
17. G. J. McKenzie, P. G. Fallon, C. L. Emson, R. K. Grencis, A. N. McKenzie, *J. Exp. Med.* **189**, 1565 (1999).
18. K. Moro *et al.*, *Nature* **463**, 540 (2010).
19. S. Nishimura *et al.*, *Nat. Med.* **15**, 914 (2009).
20. S. Winer *et al.*, *Nat. Med.* **15**, 921 (2009).
21. M. Feuerer *et al.*, *Nat. Med.* **15**, 930 (2009).
22. E. Karita *et al.*, *PLoS ONE* **4**, e4401 (2009).
23. G. S. Hotamisligil, E. Erbay, *Nat. Rev. Immunol.* **8**, 923 (2008).
24. L. Zu *et al.*, *J. Biol. Chem.* **284**, 5915 (2009).
25. V. Emilsson *et al.*, *Nature* **452**, 423 (2008).
26. Y. Chen *et al.*, *Nature* **452**, 429 (2008).

27. We thank J. Cyster, D. Erle, C. Gerard, J. Lee, and A. McKenzie for reagents and mice; N. Flores for animal husbandry; Z. Wang for technical assistance; and M. Anderson and C. Lowell for constructive review of the manuscript. This work was supported by the Howard Hughes Medical Institute and grants from the NIH (AI026918), Juvenile Diabetes Research Foundation Innovative Grant, Larry L. Hillblom Foundation Network Grant and the Sandler Asthma Basic Research Center. Support was provided by the Diabetes Endocrinology Research Center grant DK063720, UCSF Medical Scientist Training Program (D.W.), UCSF Department of Laboratory Medicine (A.B.M.), and 5F30DK083194-02 from the National Institutes of Health (D.W.). Animal care was in accordance with UCSF Laboratory Animal Resource Center committee guidelines. Mouse strains described are available upon completion of standard institutional Material Transfer Agreements.

Supporting Online Material

www.sciencemag.org/cgi/content/full/science.1201475/DC1
Materials and Methods
Figs. S1 to S9
References

9 December 2010; accepted 1 March 2011
Published online 24 March 2011;
10.1126/science.1201475

AMP-Activated Protein Kinase Regulates Neuronal Polarization by Interfering with PI 3-Kinase Localization

Stephen Amato,[1] Xiuxin Liu,[2]* Bin Zheng,[3,4]* Lewis Cantley,[3,4] Pasko Rakic,[2] Heng-Ye Man[1]†

Axon-dendrite polarization is crucial for neural network wiring and information processing in the brain. Polarization begins with the transformation of a single neurite into an axon and its subsequent rapid extension, which requires coordination of cellular energy status to allow for transport of building materials to support axon growth. We found that activation of the energy-sensing adenosine 5′-monophosphate (AMP)–activated protein kinase (AMPK) pathway suppressed axon initiation and neuronal polarization. Phosphorylation of the kinesin light chain of the Kif5 motor protein by AMPK disrupted the association of the motor with phosphatidylinositol 3-kinase (PI3K), preventing PI3K targeting to the axonal tip and inhibiting polarization and axon growth.

Morphological polarization sets the foundation for synapse formation and efficient information transfer in the brain. Polarization is initiated by the selective rapid growth of a single neurite that will eventually differentiate into an axon, whereas the remaining sister neurites become dendrites. The scale of axon growth during neuronal polarization requires both a large energy supply to support increased protein and membrane synthesis and extremely active intracellular delivery (*1*). Cellular energy status could thus be a key factor in initiating axon outgrowth and polarity formation. In all cell types, including neurons, the adenosine 5′-monophosphate (AMP)–activated protein kinase (AMPK) signaling cascade measures bio-

[1]Department of Biology, Boston University, 5 Cummington Street, Boston, MA 02215, USA. [2]Department of Neurobiology and Kavli Institute for Neuroscience, Yale University School of Medicine, New Haven, CT 06510, USA. [3]Division of Signal Transduction, Beth Israel Deaconess Medical Center, Boston, MA 02115, USA. [4]Department of Systems Biology, Harvard Medical School, Boston, MA 02115, USA.

*These authors contributed equally to this work.
†To whom correspondence should be addressed. E-mail: hman@bu.edu